DOI 10.1007/s10946-024-10188-4
Journal of Russian Laser Research, Volume 45, Number 1, January, 2024

NANOSECOND PULSE GENERATION IN THE *C*-BAND REGION USING SILVER SULFIDE AS A SATURABLE ABSORBER

Norizan Ahmed,[1*] Nur Farhanah Zulkipli,[2] Nurhaffizah Hassan,[1] Rosmawati Shafie,[1] and Syazilawati Mohamed[1]

[1] *School of Electrical Engineering, College of Engineering, Universiti Teknologi MARA Dungun 23000, Malaysia*

[2] *Department of Engineering and Built Environment Tunku Abdul Rahman University of Management and Technology (TAR UMT) Penang Branch Tanjong Bungah 11200, Pulau Pinang, Malaysia*

Corresponding author e-mail: noriz207@uitm.edu.my

Abstract

We successfully demonstrate the generation of nanosecond pulses in a passively Erbium-doped fiber laser (EDFL) by an Ag_2S-based saturable absorbeer (SA). A simple and low-cost liquid phase exfoliation (LPE) method is used to fabricate the SA. Through LPE, the SA element is coated onto a thin film of polyvinyl alcohol (PVA), which serves as the host material. The Ag_2S SA film exhibits good nonlinear absorption characteristics to give it strong potential as an ideal SA. It has a modulation depth of 25.3% and a saturation intensity of 1.11 MW/cm^2. The laser is able to generate a self-started mode-locked pulse at a threshold pump power of 145.83 mW with a fundamental repetition rate of 0.98 MHz and a pulse duration of 256 ns, respectively. At the maximum pump power, the laser delivers a pulse energy of 2.08 nJ and an output power of 2.11 mW. This demonstration suggests that Ag_2S SA has good capacity for generating nanosecond mode-locked lasers in the *C*-band region.

Keywords: passive mode locking, saturable absorber, Silver sulfide.

1. Introduction

Short-pulsed lasers are frequently used in the fields of optical communication [1], surgery [2], and laser cutting [3]. With nanosecond pulses, the potential to generate large-energy pulses is substantial. This can be achieved through active or passive techniques. Pulse generation in the active method is initiated by an acousto-optic or electro-optic modulator. By changing the resonator round-trip phase or modulating the resonator loss, the desired outcome can be achieved. However, active techniques have some limitations, such as high cost, low peak power, and low damage threshold [4]. Conversely, passive techniques utilize a saturable absorber (SA) device that can modify the resonator loss at a faster rate than the modulator, thereby resulting in shorter pulses. The use of an SA device has several advantages over the active technique, including lower-cost, simpler, and more compact systems to be realized. Additionally, Pauli's blocking principle supports the idea that the SA device is the crucial element in generating picosecond and femtosecond pulses. To significantly enhance the performance of a passively mode-locked fiber laser, it is essential to carefully select the saturable absorber (SA) materials and regulate their parameters. There are two types of SA material, real and artificial. Real SA refers to materials that display a natural nonlinear reduction in absorption as light intensity increases, while artificial SAs rely on nonlinear effects

Manuscript submitted by the authors in English on December 4, 2023.

 1071-2836/24/4501-0058

within a laser cavity to create intensity-dependent transmission and simulate the behavior of real SAs. Despite the challenges of leveraging the homogeneity of optical fiber properties for saturable absorption, real SAs are preferred for generating pulsed lasers due to their numerous advantages, such as 6he ability to be used in technical devices, wide-band operation, and fast switching speed [5].

Real SA devices can be prepared using various methods and materials, including semiconductor compounds and crystal doping; also, the mode locking was demonstrated using doped fibers. Various types of saturable absorbers have been investigated for their potential use in laser systems, including semiconductor saturable absorber mirrors (SESAMs) [6], carbon nanotubes (CNTs) [7], and graphene [8]. However, SESAMs possessed a constrained operational bandwidth, functioned exclusively within a specific wavelength range, and entailed considerably elevated expenses for fabrication and packaging [9]. On the other hand, CNTs exhibit a low damage threshold, and their operational wavelength is contingent upon the diameters of the nanotubes [10]. Additionally, graphene has a zero band gap and low modulation per layer, which restricts the potential of this saturable absorber [11]. Thus, driven by these limitations, the continuous exploration of novel saturable absorbers is necessary to identify the best candidates for achieving pulsed laser generation with good performances. Two-dimensional (2D) materials have recently been recognized for their excellent photonic properties, such as a wide range of linear optical absorption, ultrafast relaxation time, and high optical nonlinearity [12].

These properties offer numerous benefits for a wide range of potential applications in optical devices. The category of 2D materials includes a group of transition metals, namely, transition metal dichalcogenides (TMDs), transition metal chalcogenides (TMCs), and transition metal oxides (TMOs); they have been extensively studied as potential saturable absorbers (SAs) since the emergence of graphene. TMCs are a type of semiconductor material that features a sandwich-like structure. This new class of materials has several unique properties, such as a significant nonlinear optical response, a high optical damage threshold, a tunable band gap, and a high electron mobility. Ag_2S, which belongs to the TMC family, is regarded as one of the most important chalcogenides due to its small direct band gap (ranging from 0.9 to 1.05 eV), large absorption coefficient, high chemical stability, low toxicity, optical limiting properties, and unique layered structure [13, 14]. Ag_2S has shown promise as a visible–NIR photocatalyst and a complex photocatalyst in various real-time applications [15–17]. However, Ag_2S has not been thoroughly examined as a passive device, which is one of the primary reasons; it was selected as a candidate.

In this paper, our aim is to demonstrate a passively mode-locked EDFL, utilizing an Ag_2S SA material. The Ag_2S SA film is created using PVA dispersion, which is an inexpensive and straightforward method. The material demonstrates impressive saturable absorption in the *C*-band region with a saturable absorption of 25.3%, a saturation intensity of 1.11 MW/cm^2, and a nonsaturable absorption of 12.7%. These properties are determined, using a balanced twin-detector technique. By implementing the film in an Erbium-doped fiber-laser (EDFL) cavity, stable nanosecond mode-locking operations are successfully achieved.

2. Preparations of Ag_2S SA Film

The Ag_2S powder, with a molecular weight of 247.80 g/mol and a purity of 99.9% for trace metals, was purchased from Sigma Aldrich. The Ag_2S-based SA is fabricated, using the liquid phase exfoliation (LPE) method. Using LPE, the Ag_2S elements are coated on the surface of a thin film of polyvinyl alcohol (PVA), which acts as the host material. This method is simple and low-cost. First, a PVA solution is prepared by adding 1 g of PVA powder into 120 ml of distilled water, with the aid of a

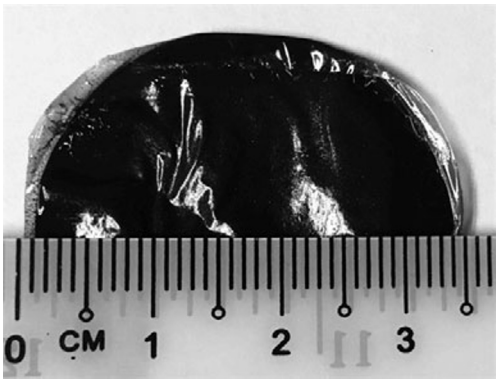

Fig. 1. The real image of the Ag_2S SA thin film.

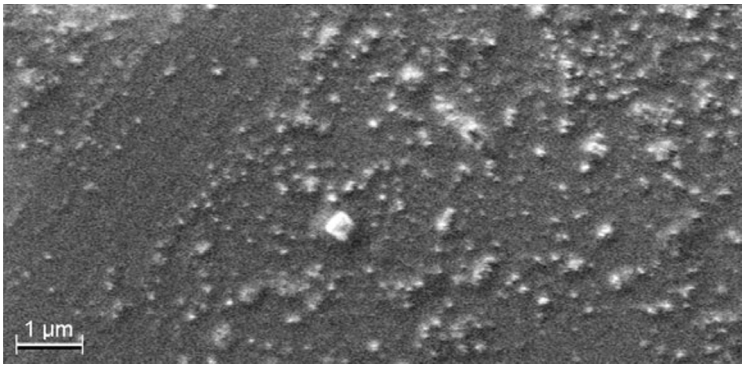

Fig. 2. FESEM image of the Ag_2S SA.

magnetic stirrer. This combining process takes about 24 h. at 300 rpm and 100°C to complete. Then, 15 mg of Ag_2S powder is added to the prepared solution, and the mixture is stirred at the same speed of 300 rpm for 12 h. To ensure thorough dissolution of the composite solution, the Ag_2S-PVA solution is then placed in an ultra-sonic bath for 1 h. Then the solution is put in a Petri dish and left to dry at room temperature for at least 48 h. This process creates a thin layer of Ag_2S-based SA film.

An actual image of the fabricated Ag_2S SA film is presented in Fig. 1. This film has an approximate thickness of 30 μm. The field-emission scanning electron microscope (FESEM) measurement depicted in Fig. 2 confirms the presence of Ag_2S particles within the PVA film. It shows that the particles are distributed evenly throughout the film. The other two images summarizes the characteristics of the SA.

In Fig. 3, we show the linear absorption profile of the Ag_2S SA film, indicating an absorption loss of approximately 3.7 dB in the 1.55 – 1.56-micrometer region. We use the technique of balanced twin-detector measurement to characterize the nonlinear absorption. To carry out the measurement, we employ a mode-locked laser source with a wavelength of 1558 nm, a repetition rate of 1.88 MHz, and a pulse width of 2.5 ps. An Erbium-doped fiber amplifier (EDFA) is used to amplify the mode-locked source. An optical attenuator is connected to the EDFA for adjusting the laser's output power. The output power is split into two equal parts, using a 3 dB coupler. The nonlinear absorption of the SA is measured by transmitting a half of the output power through the SA film and using the remaining half of the power as a reference. In Fig. 4, we display the results of the analysis, which yielded a nonsaturable absorption of 12.7%, a saturation intensity of 1.11 MW/cm^2, and a modulation depth of 25.3%.

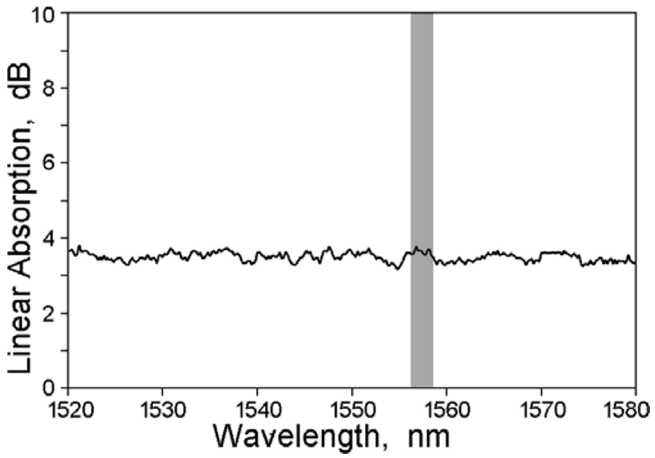

Fig. 3. The linear absorption profile of the Ag_2S thin film.

In Fig. 5, we exhibit a composition comprising 5.17% Oxygen, 20.09% Carbon, and 7.41% Sulfur, with a significant concentration of Silver exceeding 66%. These values provide evidence for the existence of Ag_2S in the film. Furthermore, the abundance of Carbon in the profile is attributed to PVA, while the

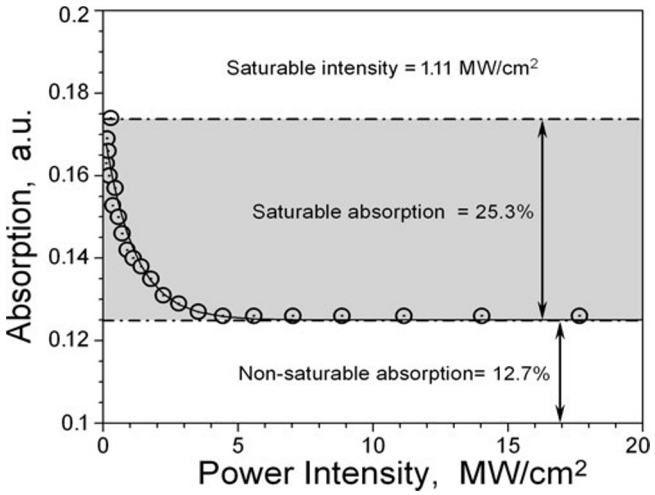

Fig. 4. The nonlinear absorption profile of the Ag_2S thin film.

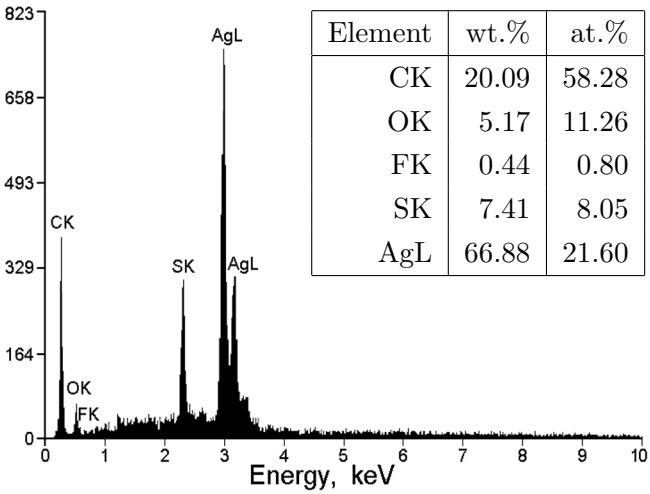

Element	wt.%	at.%
CK	20.09	58.28
OK	5.17	11.26
FK	0.44	0.80
SK	7.41	8.05
AgL	66.88	21.60

Fig. 5. EDS profile of the Ag_2S SA.

slight presence of C and O elements is due to the penetration of the thin film during the measurement process.

3. Experimental Setups

The schematic diagram of the passively mode-locked laser with an EDFL using Ag_2S-based SA is shown in Fig. 6. The experimental setup consisted of a laser diode (LD), a wavelength division multiplexer (WDM), a 2.4 m long Erbium-doped fiber (EDF) as the gain medium, an optical isolator, an SA device, and a 10 dB output coupler. The setup is configured based on a ring cavity. The EDF has a 0.24 numerical aperture, a 5.1 m core diameter, and a cladding diameter of 125.4 μm.

A laser diode with a wavelength of 974 nm is used to pump the EDF via a 980/1550 nm WDM. The isolator ensures that the light travels in only one direction within the cavity. The total length of the mode-locked EDFL cavity is approximately 207 m after adding a 200 m long standard single-mode fiber (SMF). A small piece of the Ag_2S-PVA film is cut off and attached to a fiber ferrule to form a

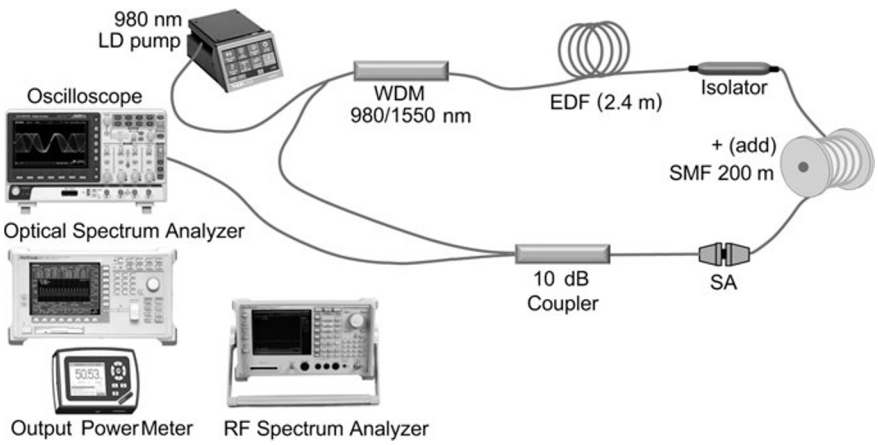

Fig. 6. Schematic diagram of the mode-locked fiber laser that uses Ag_2S SA. A single-mode fiber (SMF), that is 200 m long, is included to facilitate the mode-locking regime.

fiber-compatible SA by connecting it to a clean fiber ferrule, using a fiber adapter. A 90/10 output coupler is used to obtain 10% of the oscillating light from the cavity as the laser output. An oscilloscope (GWINSTEK: GDS-3352) and an optical spectrum analyzer (OSA: Anritsu, MS9710C, $0.6 - 1.75$ μm) are used to observe and record the pulse train and output spectrum of the laser output, respectively. To measure the repetition frequency and stability of the mode-locked lasers, an Anritsu Radio Frequency (RF) spectrum analyzer (MS2683A) operating at 7.8 GHz is used. The average output power of the pulsed laser is measured, using an output power meter (Thorlabs PM 100D).

4. Results and Discussions

In the experiment, the gain medium is pumped with a 980 nm power via WDM and, to counteract cavity dispersion, 200 m of SMF and Ag_2S SA are added to the ring cavity. Above a threshold of 145.83 mW, we achieve the stable and self-starting mode-locking regime, despite a relatively high mode-locking threshold caused by the SA's high insertion loss and long cavity. With a maximum pump power of 187.04 mW, the mode locked EDFL's optical spectrum is acquired, revealing a central peak wavelength of 1558.4 nm; see Fig. 7. Moreover, a weak Kelly sideband-like structure with low intensity is noticeable on the optical spectrum, indicating that the mode-locked laser is not functioning in the soliton regime, due to its nanosecond-range pulse duration. Nevertheless, the sidebands confirm that nonlinearity in the cavity is balanced with dispersion. The mode-locked pulse oscilloscope trace remains stable despite pump power fluctuations and environmental disturbances. The fundamental frequency correlates with a cavity length of 207 m, and the pulse width is measured to be around 230 ns at a full wave half maximum (FWHM); see Fig. 8.

After obtaining the rf spectrum at 187.04 mW pump power as shown in Fig. 9, further investigation is conducted to determine the stability of the pulsed laser. The analysis revealed a fundamental frequency of 988 kHz with at least 20 harmonics, which is consistent with the pulse period obtained from the oscilloscope trace. The trend of harmonics indicates that the mode-locking pulses are functioning in the nanosecond range. A high SNR of 69.4 dB observed in the rf spectrum indicates that the mode-locking operation is stable. To establish the role of Ag_2S SA in generating the mode-locking pulses of the laser, the Ag_2S-PVA film Is eliminated from the cavity. The fact that no pulse is detected on the oscilloscope

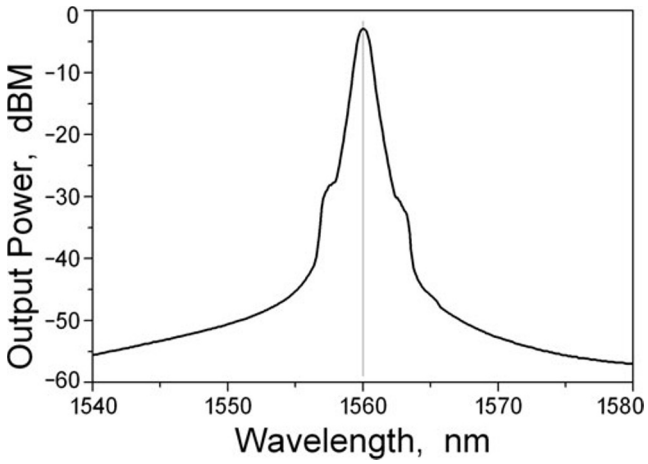

Fig. 7. The output spectrum.

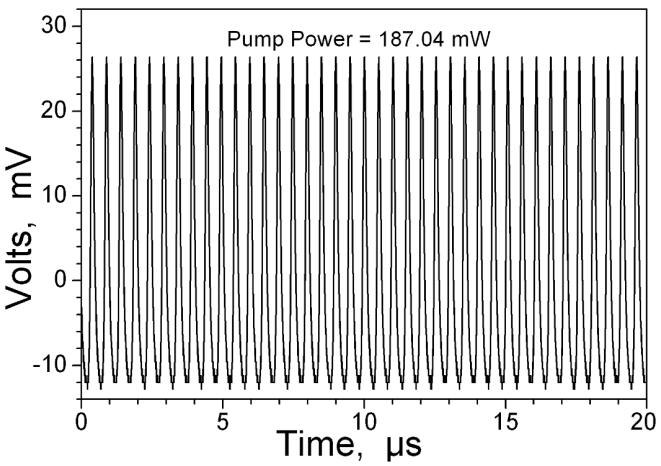

Fig. 8. The typical pulse train at the maximum pump power.

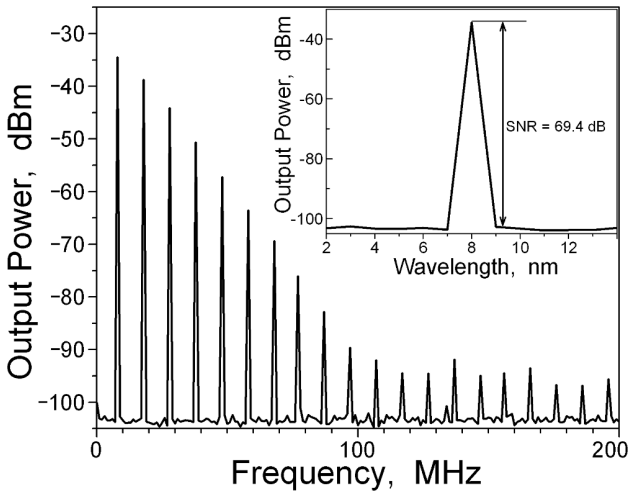

Fig. 9. The radio frequency spectrum.

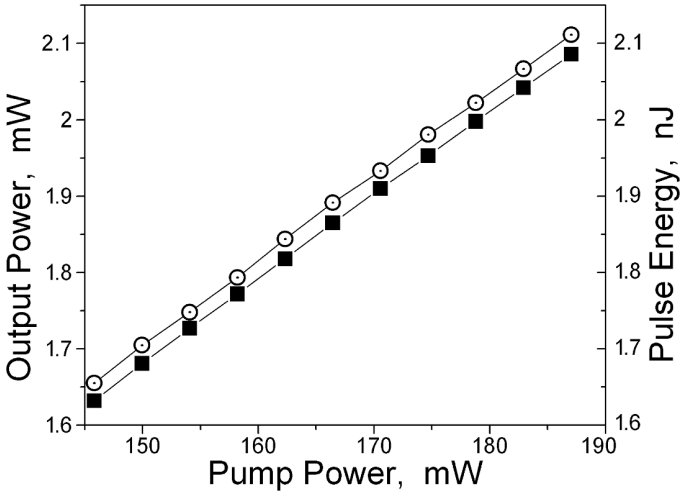

Fig. 10. The output power (⊙) and pulse energy (■) characteristics against the pump power.

throughout the pump power changes indicates that the prepared film is accountable for the pulsed laser operation.

In Fig. 10 we show the output power performance and single pulse energy at different pump power inputs. The plot shows that increasing the input pump power from 145.83 to 187.04 mW results in a linear increase in the output power from 1.63 to 2.08 mW, with a corresponding slope efficiency of 1.1%. A relatively low efficiency can be attributed to the high insertion loss of the SA. Efficiency can be improved by optimizing the cavity based on intra-cavity loss. The graph demonstrates that increase in the pump power corresponds to the increase in the pulse energy. We obtain a maximum pulse energy of 2.11 nJ at the 187.04 mW pump power. Our results show that Ag_2S material can be used as a mode-locker in an EDFL cavity for *C*-band operation.

Table 1. Comparison of the Ag_2S-Based SA's Performance to Other SAs.

SA Materials	**SA's Performance**						
	Modulation Depth, %	λ Width, nm	Repetition Rate, MHz	Pulse ns	Maximum Pulse Energy, nJ	SNR dB	Ref.
LaB_6	4.2	1559.1	1.88	157.8	5.6	73	[18]
CuNWs	8	1563.3	1.86	173	9.15	61	[19]
Sm_2O_3	33	1569.8	0.969	356	4	56	[13]
Flrpic	12.8	1562.57	3.43	120	0.33	38.3	[14]
P_3HT	11	1563	1.84	2.62	1.2	55.2	[20]
Eu_2O_3	20	1565	1.8	0.00351	1.77	70	[21]
Ag_2S	25.3	1558.4	0.988	256	2.08	69.4	This work

In Table 1, we provide a comparison of the pulse performance of the Ag_2S-based laser proposed in this study with other laser systems utilizing different saturable absorbers. The results indicate that Ag_2S exhibits a high modulation depth but a moderate pulse energy. While the modulation depth of

a saturable absorber significantly influences the efficiency of the laser system and is directly correlated with the generated pulse energy, the observed combination of high modulation depth and moderate pulse energy for Ag_2S prompts consideration of various factors within the laser system design. A higher modulation depth typically signifies a more effective saturable absorber, allowing for better control over the laser pulse characteristics. However, if a saturable absorber (SA) with a high modulation depth yields low pulse energy, it suggests potential complexities or influences from other factors in the laser system design. While a high modulation depth generally facilitates effective pulse shaping and control, other elements in the system could counteract its potential impact on the pulse energy. For example, an excessively high saturation intensity may cause the SA to saturate at relatively elevated optical power levels, thereby limiting its ability to modulate the pulses effectively. Additionally, the laser cavity design and the interaction of the saturable absorber with other cavity components can influence its performance. If the SA interacts with other optical elements in a way that diminishes its modulation effect, the pulse energy may not experience a significant increase. Moreover, the specific characteristics of the saturable absorber material, such as its recovery time, could influence its ability to modulate pulses effectively. A mismatch between the modulation depth and the material's other properties may lead to unexpected behavior.

5. Conclusions

In conclusion, using the Ag_2S-based SA, we successfully demonstrated a stable nanosecond mode-locked laser, with a modulation depth of 25.3% and a saturable optical intensity of 1.11 MW/cm^2. The passively self-started mode-locked EDFL produced a pulse width of 256 ns, a fundamental repetition rate of 988 kHz, and is centered at 1558.4 nm. The average output power and pulse energy were recorded at 2.11 mW and 2.08 nJ, respectively. The mode-locked operation demonstrated a signal-to-noise ratio (SNR) of 69.4 dB, indicating its high stability. Moreover, Ag_2S-based SA exhibited promising potential for use in developing cost-effective pulsed-laser systems operating in the *C*-band region, owing to its afford ability and simplicity.

Acknowledgments

The authors express their sincere gratitude to the diligent research team members from Universiti Teknologi Mara, Cawangan Dungun, University of Malaya and Tunku Abdul Rahman University of Management and Technology (TAR UMT) for their invaluable contributions and unwavering commitment throughout this study.

References

1. X. Hu, X. Li, Y. Zhang, et al., *Appl. Opt.*, **59**, 10 (2020).
2. Z. Li, L. Jin, and T. Gong, *Lasers Med. Sci.*, **38**, 1 (2023).
3. S. Kodama and W. Natsu, *Procedia CIRP*, **95**, 3 (2020).
4. Y. Chen, C. Zhao, and S. Chen, *IEEE J. Sel. Top. Quantum Electron.*, **20**, 5 (2014).
5. R. I. Woodward and E. J. R. Kelleher, *Appl. Sci.*, **5**, 4 (2015).
6. U. Keller, K. Weingarten, X. Franz, et al., *IEEE J. Sel. Top. Quantum Electron.*, **2**, 3 (1996).
7. Y. W. Song, S. Yamashita, and S. Maruyama, *Appl. Phys. Lett.*, **92**, 2 (2008).

8. Y. Chen, *Opt. Eng.*, **51**, 8 (2012).
9. M. Zhang, Q. Wu, F. Zhang, et al., *Adv. Opt. Mater.*, **7**, 1800224, (2019).
10. Q. Bao, H. Zhang, Y. Wang, et al., *Adv. Funct. Mater.*, **19**, 19 (2009).
11. B. Nizamani, F. Memon, Z. Umar, et al., *Optik (Stuttg).*, **219**, 4 (2020).
12. Y. N. Zhang, Z. Y. Song, D. Qiao, et al., *Nanotechnology*, **33**, 8 (2022).
13. N. F. Zulkipli, M. Batumalay, F. Samsamnun, et al., *Microw. Opt. Technol. Lett.*, **62**, 3 (2020).
14. S. Salam, A. Al-Masoodi, A. Al-Hiti, et al., *Opt. Fiber Technol.*, **50**, 3 (2019).
15. F. Wang, *Chin. Phys. B*, **26**, 3 (2017).
16. J. Feng, X. Li, Z. Shi, et al., *Adv. Opt. Mater.*, **8**, 6 (2020).
17. B. M. Al-Shehri, M. Shkir, T. M. Bawazeer, et al., *Physica E Low Dimens. Syst. Nanostruct.*, **121**, 1 (2020).
18. S. Omar, N. Zulkifli, N. Ahmed, et al., *Opt. Commun.*, **502**, 8 (2022).
19. E. I. Ismail, F. Ahmad, S. Shafie, et al., *Results Phys.*, **18**, 2 (2020).
20. F. Samsamnun, N. F. Zulkifli, M. Sarjidan, et al., *Opt. Fiber Technol.*, **54**, 11 (2019).
21. N. F. Zulkipli, A. Jafry, R. Apsari, et al., *Opt. Laser Technol.*, 127, 10 (2020).